MATERIALS PHYSICS AND MECHANICS RESEARCH ARTICLE

Submitted: November 24, 2024 **Revised: April 4, 2025** **Accepted: May 12, 2025**

Effects of post-annealing duration on the properties of β-Ga_2O_3 thin films prepared by spray pyrolysis

X. Zhang [1] ✉, D.I. Panov [1], V.A. Spiridonov [1], N.K. Kuzmenko [1], N.D. Prasolov [2], A.Yu. Ivanov [1], M.V. Dorogov [1], H.M. Wei [3], D.Y. Jiang [3], D.A. Bauman [1], A.E. Romanov [1,2,4]

[1] ITMO University, St. Petersburg, Russia

[2] Ioffe Institute, St. Petersburg, Russia

[3] School of Materials Science and Engineering, Changchun University of Science and Technology, Changchun, China

[4] ITMO/CUST Joint Institute of Mechanics and Optics, Changchun, China

✉ 314519083@qq.com

ABSTRACT

The post-annealing duration dependence of structural and optical properties of polycrystalline β-Ga_2O_3 thin films fabricated on sapphire (Al_2O_3) substrate via the spray pyrolysis method are presented. Extending the annealing time for fixed temperature 900 °C from 1 to 2 h improves crystallinity of the films, as evidenced by an increase in the average grain size approximately from 8 to 14 nm, a reduction in the full width at half maximum of the $\bar{2}02$ β-Ga_2O_3 diffraction peak from 0.43 to 0.29°. However, extending the post-annealing duration to 3 h induces excessive grain coarsening into island-like crystalline domains. These findings demonstrate that for the chosen experimental conditions, a 2-hour annealing at 900 °C represents an optimum for achieving relatively smooth and solid β-Ga_2O_3 films while balancing crystallinity and film homogeneity.

KEYWORDS

Ga_2O_3 film • spray pyrolysis • sol-gel • post-anneal • duration

***Funding**. This work was supported by the Ministry of Science and Higher Education of the Russian Federation, project no. FSER-2025-0005. X. Zhang was supported by the China Scholarship Council. A.E. Romanov was also supported by Foreign Experts Key Support Project (Northeast Special Project), Grant No. D20240015 for his work in China on theoretical analysis of the obtained results.*

Citation: Zhang X, Panov DI, Spiridonov VA, Kuzmenko NK, Prasolov ND, Ivanov AYu, Dorogov MV, Wei HM, Jiang DY, Bauman DA, Romanov AE. Effects of post-annealing duration on the properties of β-Ga_2O_3 thin films prepared by spray pyrolysis. *Materials Physics and Mechanics*. 2025;53(2): 55–63.
http://dx.doi.org/10.18149/MPM.5322025_6

Introduction

Gallium oxide (Ga_2O_3), particularly its thermodynamically stable monoclinic β-phase, emerged as a promising ultra-wide bandgap semiconductor for next-generation power electronics and deep-ultraviolet (UV) optoelectronic devices [1]. With a bandgap of ~ 4.9eV, β-Ga_2O_3 exhibits exceptional properties, including a high breakdown electric field (8 MV/cm), Baliga's figure of merit (BFOM = $\varepsilon \cdot \mu \cdot E_c^3$, where ε is relative dielectric constant, μ is electron mobility and E_c is critical electric field) (3444), and thermal stability up to its melting point (~1795 °C) [2–4]. These characteristics position Ga_2O_3 as a superior alternative to the conventional semiconductors like SiC and GaN in high-voltage, high-

Publisher: Peter the Great St. Petersburg Polytechnic University

temperature applications such as solar-blind photodetectors, Schottky diodes, and MOSFETs [1,2]. However, the performance of β-Ga_2O_3 thin films is critically dependent on their crystallinity, stoichiometry, and defect density, which are strongly influenced by synthesis methods and post-processing.

Thin-film fabrication techniques for β-Ga_2O_3 include molecular beam epitaxy (MBE) [5], pulsed laser deposition (PLD) [6], chemical vapor deposition (CVD) [7], metalorganic vapor-phase epitaxy (MOVPE) [8], halide vapor phase epitaxy (HVPE) [9], and radio frequency magnetron sputtering (RFMS) [10,11]. While these methods yield high-quality epitaxial layers, they suffer from limitations such as high equipment costs, complex vacuum requirements, and limited scalability. In contrast, sol-gel methods [12,13] like spray pyrolysis [14,15] offer cost-effective, scalable alternatives. The sol-gel technique excels in molecular-level homogeneity and precise doping control, enabling uniform incorporation of dopants such as Al [16] or Sn [17] to tailor optical and electrical properties. Spray pyrolysis, on the other hand, combines simplicity with industrial scalability, allowing large-area deposition at atmospheric pressure.

Post-annealing is a critical step in optimizing the structural and functional properties of solution-processed Ga_2O_3 films [18,19]. Thermal treatment facilitates the decomposition of organic residues, enhances crystallinity by promoting phase transitions, and mitigates defects such as oxygen vacancies [20,21]. This work investigates the effects of post-annealing duration on the properties of β-Ga_2O_3 thin films fabricated via spray pyrolysis method on sapphire substrate. By correlating annealing time with structural evolution, surface morphology, and optoelectronic performance, we aim to establish optimal processing parameters for high-performance devices.

Materials and Methods

β-Ga_2O_3 thin films were synthesized on (0001)-oriented sapphire (Al_2O_3) substrate via a particular variant of sol-gel technique, namely, spray pyrolysis method. The precursor solution was formulated using gallium nitrate hydrate [$Ga(NO_3)_3{\cdot}8H_2O$, 99.9 %, Lankhit] dissolved in 2-methoxyethanol [$C_3H_8O_2$, 99.5 %, Leap Chem], serving as the solvent. Monoethanolamine (MEA) [C_2H_7NO, 99.5 %, Vekton] was introduced as a stabilizer to ensure solution homogeneity and prevent premature precipitation. The molar concentrations of both gallium nitrate and 2-methoxyethanol were maintained at 0.25 mol/L, with a 3:1 molar ratio of gallium nitrate to MEA. The mixture was magnetically stirred at 60 °C for 1 h to achieve a pale yellow, transparent and stable sol. Prior to deposition, the (0001) sapphire substrate underwent ultrasonic cleaning in sequential baths of isopropanol and deionized water (10 min each) to remove organic contaminants and particulate matter.

The spray pyrolysis setup for Ga_2O_3 thin film fabrication has been described in detail in our previous work [14]. Figure 1 illustrates the preparation workflow. The sol was sprayed onto substrates mounted on a heating stage maintained at 140 °C. Following solvent evaporation, the samples were transferred to a preheated muffle furnace and pre-annealed at 500 °C for 10 min under ambient air atmosphere. This deposition-pre-annealing cycle was repeated 30 times to achieve the desired film thickness. After fabrication, the samples were subjected to post-annealing in the same muffle furnace

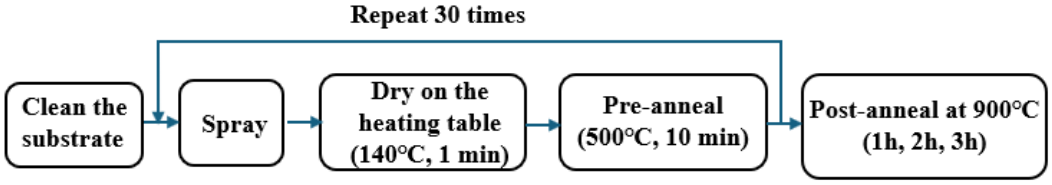

Fig. 1. The workflow of Ga_2O_3 films fabricated by spray pyrolysis

at 900 °C (this temperature corresponds to experimental results published in [21,22]) in air with varying durations of 1, 2, and 3 h.

The crystal structure of the samples was characterized using a Rigaku Ultima IV X-ray diffractometer (XRD) with Cu-Kα radiation (λ = 0.15418 nm). XRD patterns were acquired in the 2ϑ angular range of 25 to 70° at a scanning rate of 0.5°/min.

The average crystallite size, representing the coherent scattering domain, was determined through Halder-Wagner analysis [23,24] of the XRD data using the following relation:

$$\left(\frac{\beta^*}{d^*}\right)^2 = \frac{1}{t} \times \left(\frac{\beta^*}{d^{*2}}\right) + \left(\frac{\varepsilon}{2}\right)^2, \quad (1)$$

where $\beta^* = \frac{\beta cos\theta}{\lambda}$, $d^* = \frac{2sin\theta}{\lambda}$, β denotes the experimental FWHM (in radians), λ = 0.15418 nm (Cu-Kα radiation wavelength), ε quantifies the micro-strain within crystallites, t corresponds to the average crystallite size.

The surface morphology of the films was characterized using a TESCAN Mira 3 scanning electron microscope (SEM). For quantitative surface roughness analysis, a Veeco Dimension 3100 atomic force microscope (AFM) was employed to measure the root-mean-square (RMS) roughness and map nanoscale topographic features.

The optical properties of the β-Ga_2O_3 thin films were investigated through transmittance spectroscopy and Tauc plot analysis [25]. Optical transmission spectra were acquired in the 200–850 nm wavelength range using a PerkinElmer Lambda 950 UV-Vis-NIR spectrophotometer, with (0001)-oriented sapphire substrates serving as optical windows. Film thickness was determined via cross-sectional SEM imaging. The optical bandgap (E_g) was calculated using the Tauc relation [25]:

$$(\alpha h\nu)^2 = A(h\nu - E_g), \quad (2)$$

where α is the absorption coefficient, $h\nu$ represents photon energy, and A is a proportionality constant.

The influence of post-annealing temperature on surface morphology and optoelectronic properties was systematically evaluated through comparative analysis of structural and optical data.

Results and Discussion

Figure 2 shows the XRD spectra of β-Ga_2O_3 films post-annealed at 900 °C for 1, 2, and 3 h. Four significant reflection peaks are observed at 30.2, 31.6, 59.3, and 64.7°, corresponding to the (400), $(\bar{2}02)$, $(\bar{6}03)$, and $(\bar{7}12)$ crystallographic planes of crystallites in β-Ga_2O_3 polycrystalline film, respectively. With the increase of post-annealing duration, the intensity of the $\bar{2}02$ peak is significantly enhanced and its FWHM decreases, while the other main peaks do not change significantly. This selective enhancement of the

contribution of $(\bar{2}02)$ orientation can be attributed to the synergistic effect between substrate-induced epitaxial orientation and thermally activated grain reorganization. The (0001) surface of sapphire substrate has a hexagonal close-packed structure and has a template effect, which is conducive to the growth of β-Ga_2O_3 grains along a specific crystallographic direction. The $(\bar{2}02)$ facet of β-Ga_2O_3 may show good lattice matching with the substrate, thus minimizing the interface energy and promoting the preferred orientation during post-annealing.

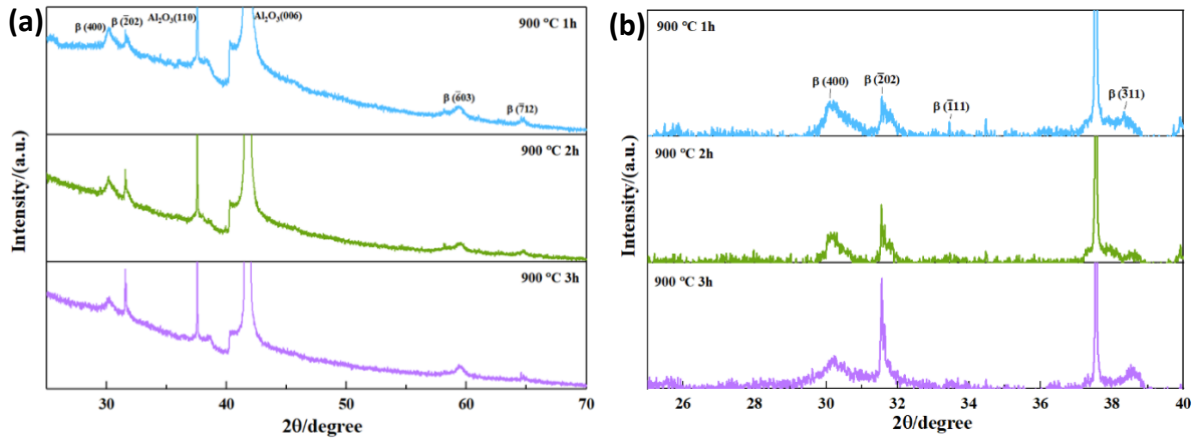

Fig. 2. XRD patterns of β-Ga_2O_3 thin films post-annealed at 900 °C for durations of 1, 2, and 3 h (a), detailed patterns (b), compared with ICDD reference data (PDF 00-041-1103)

Table 1 summarizes the analysis of diffraction peaks for β-Ga_2O_3 thin films post-annealed at 900 °C for 1, 2, and 3 h. Initially, increasing the annealing duration from 1 to 2 h resulted in a reduction of the full width at half maximum (FWHM) for $\bar{2}02$ peak from 0.43 to 0.29°, accompanied by an increase in average crystallite size from 8.15 to 14.06 nm. This behavior is consistent with enhanced crystallinity and grain coarsening, aligning with classical Ostwald ripening [26], where smaller grains dissolve to supply larger ones, thereby reducing lattice defects and micro-strains. However, extending the annealing time to 3 h further reduces the full width at half maximum (FWHM) to 0.13°, while decreasing the average crystallite size to 11.44 nm. This behavior of the average grain size contradicts the traditional mechanism of nucleation during film crystallization from the amorphous state. Similar effects were observed in other studies [21,27]. In part, this behavior of the grain size can be explained by processes similar to sintering, when additional formation of small grains occurs in the pores between large grains. This can lead to a decrease in the average grain size at a certain stage. Another reason may be the diffusion of aluminum from the substrate, which is observed at temperatures of 900–1000 °C [27,28]. Due to diffusion, a double solid solution $(Al_xGa_{1-x})_2O_3$ can form in the region close to the substrate, which can also lead to a decrease in the average grain size [29]. However, these hypotheses require verification and confirmation by independent experiments, as well as the dependence of the grain size on the annealing time.

Figure 3 shows top-view SEM images of β-Ga_2O_3 films post-annealed at 900 °C for 1, 2, and 3 h, showing the evolution of the film surface morphology and grain structure under different heat treatment durations. For the sample post-annealed for 1 h (Fig. 3(a)), the film surface is relatively smooth and uniform, and the grains are small and

Table 1. Diffraction peak analysis of β-Ga_2O_3 films with post-annealing temperature of 900 °C and time of 1, 2, and 3 h

Duration, h	FWHM of $\bar{2}02$ peak, °	Average crystallite size, nm
1	0.43	8.15
2	0.29	14.06
3	0.13	11.44

loosely distributed. This indicates that the grain growth is limited in the initial stage of post-annealing because the thermal energy is insufficient for significant atomic diffusion. When the time is extended to 2 h (Fig. 3(b)), the grain density and uniformity are significantly improved, and directional texture appears on the surface. This texture may be aligned with the crystal plane orientations, reflecting the enhancement of atomic mobility and stress relaxation during long post-annealing. For the sample post-annealed for 3 h (Fig. 3(c)), the grain clusters are significantly coarsened to form irregularly sized crystal islands, and the directional texture disappears, which is the result of the combined effects of competitive grain growth mechanisms or local strain redistribution.

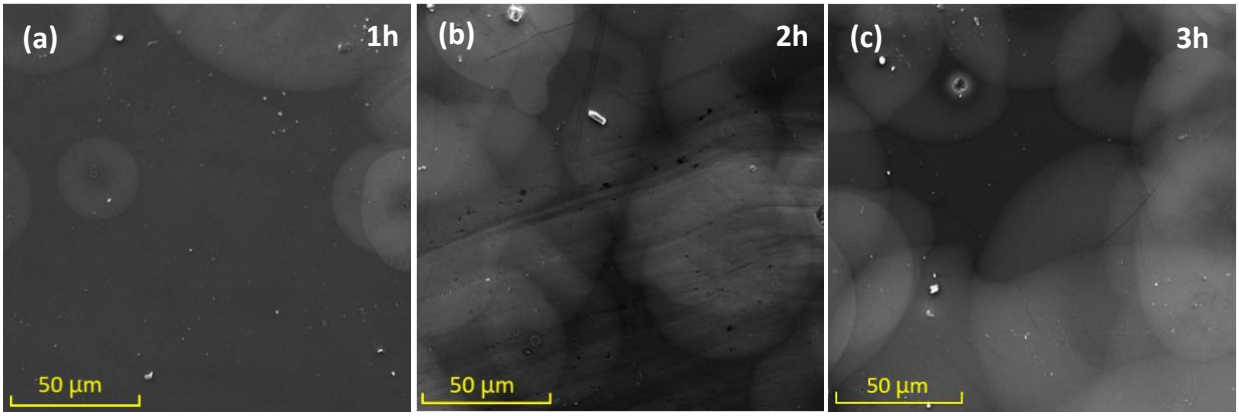

Fig. 3. SEM top-view images of β-Ga_2O_3 films post-annealed at 900 °C for (a) 1, (b) 2, (c) 3 h

Side-view SEM images of β-Ga_2O_3 films post-annealed at 900 °C for 1, 2, and 3 h are shown in Fig. 4. The thickness of all samples is from 1 to 1.1 µm, demonstrating that the annealing time has little effect on the film thickness. For the sample post-annealed for 1 h (Fig. 4(a)), the film exhibits a relatively discontinuous layered structure. The grain boundaries are not resolved and the interface between the film and the substrate is slightly rough, indicating incomplete crystallization and limited atomic mobility in the initial stage of post-annealing. This is because the oxygen vacancy compensation effect is stronger than grain growth in a shorter post-annealing time, and insufficient stored thermal energy will limit the complete densification of the film. When the post-annealing time is increased to 2 h (Fig. 4(b)), a more uniform and continuous film cross section structure is observed, accompanied by neatly arranged columnar grains, indicating that atomic diffusion and micro-stress relaxation are enhanced. For the 3 h post-annealed sample (Fig. 4(c)), the columnar grains evolved into larger irregularly shaped domains. This overgrowth and partial structural degradation indicate that the grain growth mechanism shifted from controlled grain growth to competitive crystallization, and excessive thermal exposure led to local micro-strain accumulation.

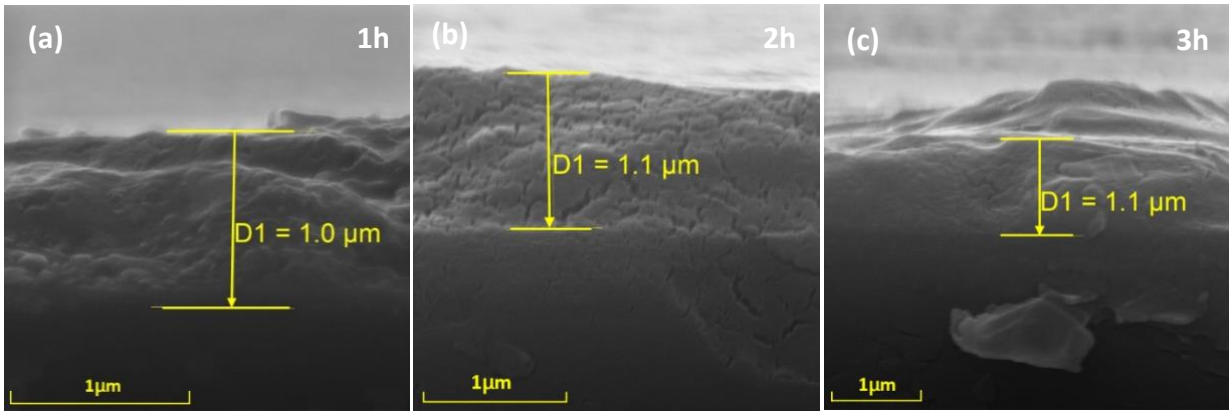

Fig. 4. SEM side-view images of β-Ga_2O_3 films post-annealed at 900°C for (a) 1, (b) 2, (c) 3 h

The two-dimensional AFM images (1 × 1 μm^2) of β-Ga_2O_3 films with different post-annealing durations were analyzed using AFM. As shown in Fig. 5, the surface of the film post-annealed for 1 h is smooth and uniform, with sparse grain distribution and the RMS roughness of 0.94 nm. When the post-annealing duration is extended to 2 h, a significant increase in grain density and size is observed, and the closely packed grains coalesce into a continuous and dense film structure. RMS roughness corresponding to this morphological transformation increases to 1.87 nm. This result is consistent with the increase in the average grain size (see Table 1). Further extending the post-annealing duration to 3 h will form heterogeneous crystal islands of various sizes, and the RMS roughness increases significantly to 2.54 nm. This change is due to thermally driven atomic reorganization. Initially, extending the post-annealing duration is beneficial for the migration of gallium and oxygen atoms to energetically favorable lattice positions, thereby enhancing the densification and crystallinity of the film [30]. However, over-annealing will destroy this balance. This process leads to non-uniform grain growth and competitive crystallization, which increases surface roughness, size differences, and spatial inhomogeneity of grain distribution. Therefore, prolonged thermal exposure can compromise the homogeneity of the structure.

Figure 6 shows the transmittance and estimated band gap of β-Ga_2O_3 films post-annealed at 900 °C for 1, 2, and 3 h. The transmittance of the samples is about 90 % in the 300–850 nm range and has sharp absorption band edges near 250 nm. As the post-annealing

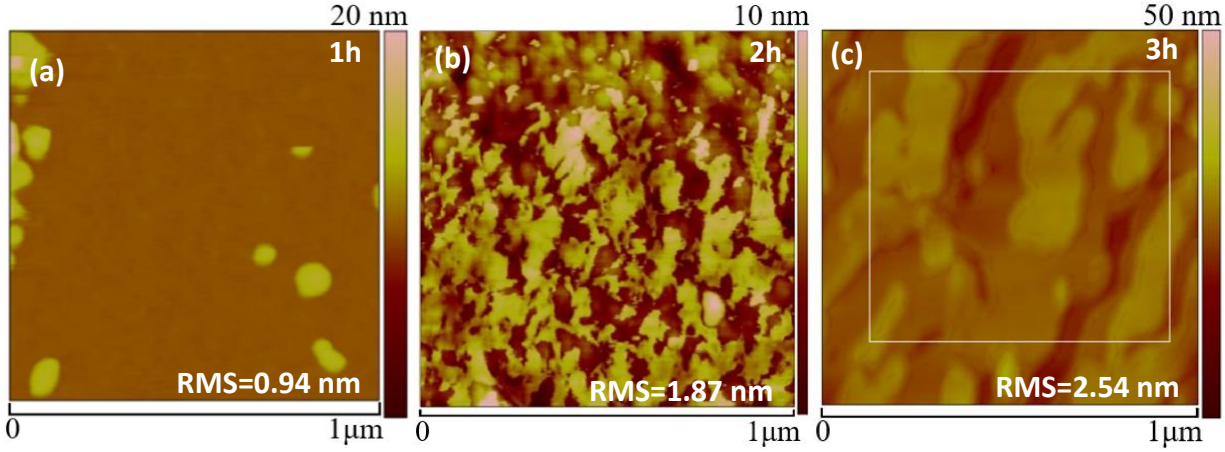

Fig. 5. AFM images of β-Ga_2O_3 films post-annealed at 900 °C for (a) 1, (b) 2, (c) 3 h

time increases, the measured optical band gap values are 4.98, 4.93, and 4.95 eV. The change in the band gap width may be associated with the corresponding changes in the micro-stresses in the film, discussed above. Concurrently, the extended post-annealing duration can facilitate diffusion-driven incorporation of Al^{3+} ions from the (0001) Al_2O_3 substrate into Ga^{3+} lattice positions within the β-Ga_2O_3 lattice sites. This may lead to the formation of a double solid solution of $(AlGa)_2O_3$ in the near-substrate region, the band gap width of which is larger than that of gallium oxide, proportional to the aluminum content [31]. However, the observed variations in the band gap width are too small to confidently draw conclusions about any noticeable trend.

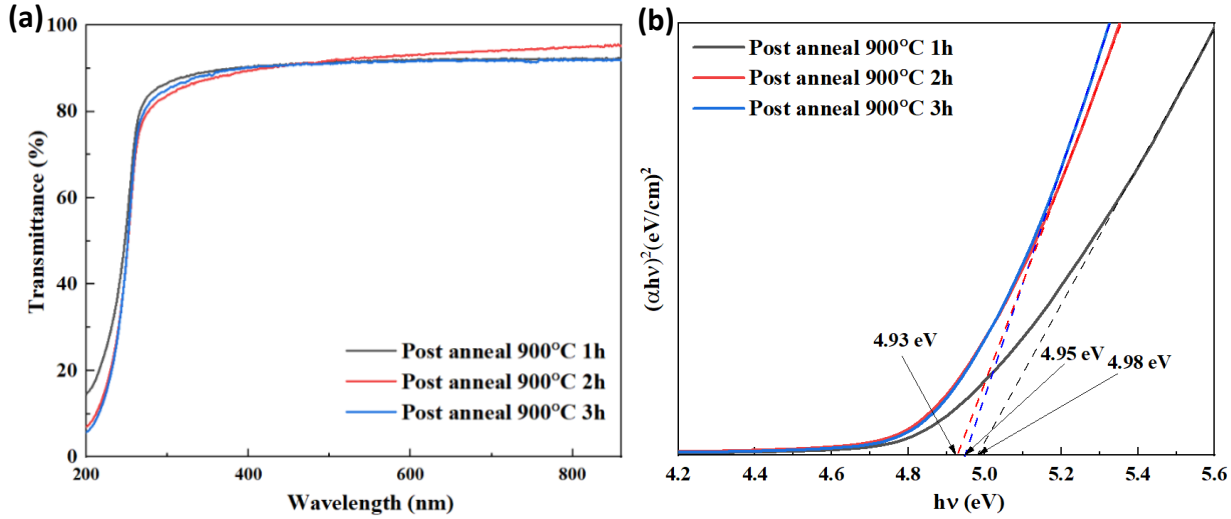

Fig. 6. (a) Optical transmission spectra and (b) bandgap estimation of β-Ga_2O_3 films post-annealed at 900 °C for 1, 2, 3 h

Conclusions

In this study we have systematically investigated the structural evolution and optic properties of spray-pyrolyzed β-Ga_2O_3 thin films as function of post-annealing duration (1–3 h at 900 °C). Increasing the post-annealing duration from 1 to 2 h enhances crystallinity, as evidenced by the growth of the average grain size from 8.15 to 14.06 nm, a reduction in the FWHM of the $\bar{2}02$ peak from 0.43 to 0.29°, and an increase in the RMS surface roughness from 0.94 to 1.87 nm. Concurrently, stress relaxation mediated by grain boundary migration narrows the optical bandgap from 4.98 to 4.93 eV. However, extending the post-annealing duration to 3 h further reduces the FWHM of the $\bar{2}02$ peak to 0.13°, while decreasing the average grain size to 11.44 nm and elevating the RMS surface roughness to 2.54 nm. This suggests that prolonged post-annealing triggers competitive grain growth, leading to heterogeneous coarsening into island-like crystalline domains.

The obtained results underscore that moderate post-annealing duration (2 h) optimizes crystallinity, whereas excessive thermal exposure compromises structural homogeneity. This study establishes that under the chosen experimental conditions, a 2-hour post-annealing at 900 °C represents an optimum for obtaining relatively smooth and solid β-Ga_2O_3 thin films. These findings advance the development of cost-effective,

scalable Ga_2O_3-based technologies, effectively bridging the gap between laboratory-scale synthesis and industrial applications.

CRediT authorship contribution statement

Xi Zhang : writing – original draft, conceptualization, investigation, data curation; **Dmitrii I. Panov**: data curation; **Vladislav A. Spiridonov**: data curation; **Natalia K. Kuzmenko**: data curation; **Nikita D. Prasolov**: data curation; **Andrey Yu. Ivanov** : data curation; **Maksim V. Dorogov** : data curation; **Haoming Wei** : investigation; **Dayong Jiang**: investigation; **Dmitrii A. Bauman**: writing – review & editing, supervision; **Alexey E. Romanov**: supervision.

Conflict of interest

The authors declare that they have no conflict of interest.

References

1. Pearton SJ, Yang J, Cary PH, Ren F, Kim J, Tadjer MJ, Mastro MA. A review of Ga_2O_3 materials, processing, and devices. *Applied Physics Reviews.* 2018;5(1): 011301.
2. Stepanov SI, Nikolaev VI, Bougrov VE, Romanov AE. Gallium oxide: properties and applications - a review. *Reviews on Advanced Materials Science.* 2016;44(1): 63–86.
3. Liu Z, Li PG, Zhi YS, Wang XL, Chu XL, Tang WH. Review of gallium oxide based field-effect transistors and schottky barrier diodes. *Chinese Physics B.* 2019;28(1): 017105.
4. Schneider SJ, Waring JL. Phase equilibrium relations in the Sc_2O_3-Ga_2O_3 System. *Journal of Research of the National Bureau of Standards-A. Physics and Chemistry.* 1963;67A(1): 19–25.
5. Oshima T, Okuno T, Fujita S. Ga_2O_3 thin film growth on c-plane sapphire substrates by molecular beam epitaxy for deep-ultraviolet photodetectors. *Japanese Journal of Applied Physics.* 2007;46(11): 7217–7220.
6. Xu C, Shen L, Liu H, Pan X, Ye Z. High-quality β-Ga_2O_3 films with influence of growth temperature by pulsed laser deposition for solar-blind photodetectors. *Journal of Electronic Materials.* 2021;50(4): 2043–2048.
7. Rafique S, Han L, Zhao H. Synthesis of wide bandgap Ga_2O_3 (E_g ~ 4.6-4.7 eV) thin films on sapphire by low pressure chemical vapor deposition. *Physica Status Solidi (a).* 2016;213(4): 1002–1009.
8. Tadjer MJ, Mastro MA, Mahadik NA, Currie M, Wheeler VD, Freitas JA, Greenlee JD, Hite JK, Hobart KD, Eddy CR, Kub FJ. Structural, optical, and electrical characterization of monoclinic β-Ga_2O_3 grown by MOVPE on sapphire substrates. *Journal of Electronic Materials.* 2016;45(4), 2031–2037.
9. Murakami H, Nomura K, Goto K, Sasaki K, Kawara K, Thieu QT, Togashi R, Kumagai Y, Higashiwaki M, Kuramata A, Yamakoshi S, Monemar B, Koukitu A. Homoepitaxial growth of β-Ga_2O_3 layers by halide vapor phase epitaxy. *Applied Physics Express.* 2015;8(1): 015503.
10. Yue W, Yan J, Wu J, Zhang L. Structural and optical properties of Zn-doped β-Ga_2O_3 films. *Journal of Semiconductors.* 2012;33(7): 073003.
11. Mohammed AAA, Lim WF. Effects of implementing dual-step nitrogen ambient for growth and post-deposition annealing of Ga_2O_3 films sputtered on silicon. *Journal of Materials Science: Materials in Electronics.* 2024;35: 1763.
12. Hench LL, West JK. The sol-gel process. *Chemical Reviews.* 1990;90(1): 33–72.
13. Zhu Y, Xiu X, Cheng F, Li Y, Xie Z, Tao T, Chen P, Liu B, Zhang R, Zheng YD. Growth and nitridation of β-Ga_2O_3 thin films by sol-gel spin-coating epitaxy with post-annealing process. *Journal of Sol-Gel Science and Technology.* 2021;100: 183–191.
14. Panov DI, Zhang X, Spiridonov VA, Azina LV, Nuryev RK, Prasolov ND, Sokura LA, Bauman DA, Bougrov VE, Romanov AE. Thin films of gallium oxide obtained by spray-pyrolysis: method and properties. *Materials Physics and Mechanics.* 2022;50(1): 107–117.
15. Ouadah E, Hamdadou N. Synthesis of WO2.72:Fe thin films via ammonium tungstate precursor by spray pyrolysis technique and annealing. *Materials Physics and Mechanics.* 2024;52(4): 141–151.

16. Tang X, Li KH, Liao CH, Vasquez JMT, Wang C, Xiao N, Li X. Chemical solution deposition of epitaxial indium- and aluminum-doped Ga_2O_3 thin films on sapphire with tunable bandgaps. *Journal of the European Ceramic Society.* 2022;42(1): 175–180.
17. Li Y, Li Y, Ji Y, Wang H, Zhong D. Sol–gel preparation of Sn doped gallium oxide films for application in solar-blind ultraviolet photodetectors. *Journal of Materials Science.* 2022;57: 1186–1197.
18. Kaminskii VV, Panov DYu, Spiridonov VA, Bauman DA, Kalganov DA, Scheglov MP, Romanov AE. Effect of high-temperature annealing on the internal friction and optical transmittance of single crystal gallium oxide. *Materials Physics and Mechanics.* 2024;52(5): 48–54.
19. Spiridonov VA, Panov DI, Ivanov AYu, Bauman DA, Romanov AE. The effect of high-temperature annealing on the properties of bulk β-Ga2O3 obtained in different growth atmospheres. *Materials Physics and Mechanics.* 2024;52(3): 80–85.
20. Rafique S, Han L, Zhao H. Thermal annealing effect on β-Ga_2O_3 thin film solar blind photodetector hetero epitaxially grown on sapphire substrate. *Physica Status Solidi (a).* 2017;214(8): 1700063.
21. Bae MS, Kim SH, Baek JS, Koh JH. Comparative study of high-temperature annealed and RTA process β-Ga_2O_3 thin film by sol–gel process. *Coatings.* 2021;11(10): 1220.
22. Zhang X, Jiang DY, Zhao M, Zhang HX, Li MY, Xing MJ, Han JC, Romanov AE. The effect of annealing temperature on Ga_2O_3 film properties. *Journal of Physics: Conference Series.* 2021;1965: 012066.
23. Nath D, Singh F, Das R. X-Ray diffraction analysis by Williamson-Hall, Halder-Wagner and size-strain plot methods of CdSe nanoparticles- a comparative study. *Materials Chemistry and Physics.* 2020;239: 122021.
24. Halder NC, Wagner CNJ. Separation of particle size and lattice strain in integral breadth measurements. *Acta Crystallographica.* 1966;20(2): 312–313.
25. Sangiorgi N, Aversa L, Tatti R, Verucchi R, Sanson A. Spectrophotometric method for optical band gap and electronic transitions determination of semiconductor materials. *Optical Materials.* 2017;64: 18–25.
26. Baldan A. Review progress in Ostwald ripening theories and their applications to nickel-base superalloys Part I: Ostwald ripening theories. *Journal of Materials Science.* 2002;37: 2171–2202.
27. Hu H, Liu Y, Han G, Fang C, Zhang Y, Liu H, Wang Y, Liu Y, Ye J, Hao Y. Effects of post annealing on electrical performance of polycrystalline Ga_2O_3 photodetector on sapphire. *Nanoscale Research Letters.* 2020;15(1): 100.
28. Goyal A, Yadav BS, Thakur OP, Kapoor AK, Muralidharan R. Effect of annealing on β-Ga_2O_3 film grown by pulsed laser deposition technique. *Journal of Alloys and Compounds.* 2014; 583: 214–219.
29. Rubio EJ, Mates TE, Manandhar S, Nandasiri M, Shutthanandan V, Ramana CV. Tungsten incorporation into gallium oxide: crystal structure, surface and interface chemistry, thermal stability, and interdiffusion. *The Journal of Physical Chemistry C.* 2016;120(47): 26720–26735.
30. Dong L, Jia R, Xin B, Zhang Y. Effects of post-annealing temperature and oxygen concentration during sputtering on the structural and optical properties of β-Ga_2O_3 films. *Journal of Vacuum Science & Technology A.* 2016;34(6): 060602.
31. Zakgeim D, Bauman D, Panov D, Spiridonov V, Kremleva A, Smirnov A, Odnoblyudov M, Romanov A, Bougrov V. Growing of bulk β-$(Al_xGa_{1-x})_2O_3$ crystals from the melt by Czochralski method and investigation of their structural and optical properties. *Applied Physics Express.* 2022;15(2): 025501.